

Evaluation of TerraSAR-X DINSAR and IPTA for ground-motion monitoring

Urs Wegmüller¹, Diana Walter², Volker Spreckels³, and Charles Werner¹

¹Gamma Remote Sensing AG, CH-3073 Gümligen, Switzerland

²TU Clausthal, Institute of Geotechnical Engineering and Mine Surveying, D-38678 Clausthal-Zellerfeld, Germany

³RAG Aktiengesellschaft, RAG Deutsche Steinkohle, Dept. BG G, D-44623 Herne, Germany

Abstract

An important objective of the Pre-Launch AO Project GEO_165 is the evaluation of TerraSAR-X time series for ground-motion monitoring. For this purpose we ordered a significant series of TerraSAR-X repeat observations in fine resolution, single polarization stripmap mode. For the selected site there is a real monitoring demand and SAR interferometry shall play an important role in the integrated monitoring concept. SAR data of other sensors (ASAR, PALSAR) are also acquired over this site offering possibilities for comparisons. The interferometric analysis is supported by ground-based measurement campaigns (leveling, realtime, static and permanent GPS) and corner reflector installation. Differential SAR interferometry (DINSAR) and Interferometric Point Target Analysis (IPTA) are used to monitor ground movements in selected parts of a German mining area.

1. Introduction

The work presented in this paper was conducted in the frame of the TerraSAR-X Pre-launch AO Project GEO_165 (PI Urs Wegmüller). This investigation is conducted in the frame of the RAG R&D project GEOMON (FE0572-0000) and RFCS2007-Project PRESIDENCE (RFCS-CT-2007-00004) of the Research Programme of the Research Fund for Coal and Steel (RFCS-CT).

The objective of this paper is to discuss SAR data processing issues and as well as some results achieved using TerraSAR-X data.

An important objective of the Pre-Launch AO Project GEO_165 is the evaluation of TerraSAR-X time series for ground-motion monitoring. For this purpose we ordered a significant series of TerraSAR-X repeat observations in fine resolution, single polarization stripmap mode. For the selected site there is a real monitoring demand and SAR interferometry shall play an important role in the integrated monitoring concept. SAR data of other sensors (ASAR, PALSAR) are also acquired over this site offering possibilities for comparisons. The interferometric analysis is supported by ground-based measurement campaigns (leveling, realtime, static and permanent GPS) and corner reflector installation. Differential SAR interferometry (DINSAR) and Interferometric Point Target Analysis (IPTA) are used to monitor ground movements in selected parts of a German mining area. Until November 2008 more than 20 scenes were acquired over our test-site, so that we are also in the position to present initial results from our persistent scatterer interferometry (PSI) analysis.

2. Data programming, ordering and delivery

The TerraSAR-X data were programmed and ordered using the online system of DLR. Given the many different modes of the SAR instrument it is an absolute requirement to program the data before the acquisition – without programming no time series data suited for interferometry would be available. The following descending scenes were programmed (up to October 2008) for the site Ruhrgebiet (Strip 012R) with incidence angle range of 39-42° using the online system of DLR (crossed out dates were ordered but not acquired):

11-Feb-2008	26-Mar-2008	09-May-2008	22-Jun-2008	05-Aug-2008	18-Sep-2008
22-Feb-2008	06-Apr-2008	20-May-2008	03-Jul-2008	16-Aug-2008	29-Sep-2008
04-Mar-2008	17-Apr-2008	31-May-2008	14-Jul-2008	27-Aug-2008	10-Oct-2008
15-Mar-2008	28-Apr-2008	11-Jun-2008	25-Jul-2008	07-Sep-2008	21-Oct-2008

3. SLC data co-registration, multi-looking, geocoding

The TerraSAR-X data obtained were single-look complex (SLC) data with pixel spacings of 1.36m in slant-range and 1.90m in azimuth. As SLC reference geometry we used the first scene which was acquired (11-Feb-2008). Geocoding was performed on the multi-look intensity image of the reference scene. From the geocoding we also obtained the terrain heights in SAR geometry. These terrain heights were considered in the SLC co-registration. The co-registration approach included also a refinement step using actual offset estimates between the data sets and it provides error statistics. Offsets determined in a test for the co-registered SLCs showed a very low standard deviation below 0.05 SLC pixel.

4. Differential interferogram generation

In a next step we generated differential interferograms for all combinations and the entire area. This was done for several reasons that included:

- estimation of orbital phase trends
- get experience on dependence of coherence on ground cover, baseline and time interval
- get experience with level, spatial scale, and location of deformation, atmospheric effects, and other phase effects (e.g. caused by DEM errors)
- data quality checking

An example of such a “survey differential interferogram” is shown in Figure 1. A low spatially low-frequency component of the phase was estimated and subtracted to better identify significant local phase gradients.

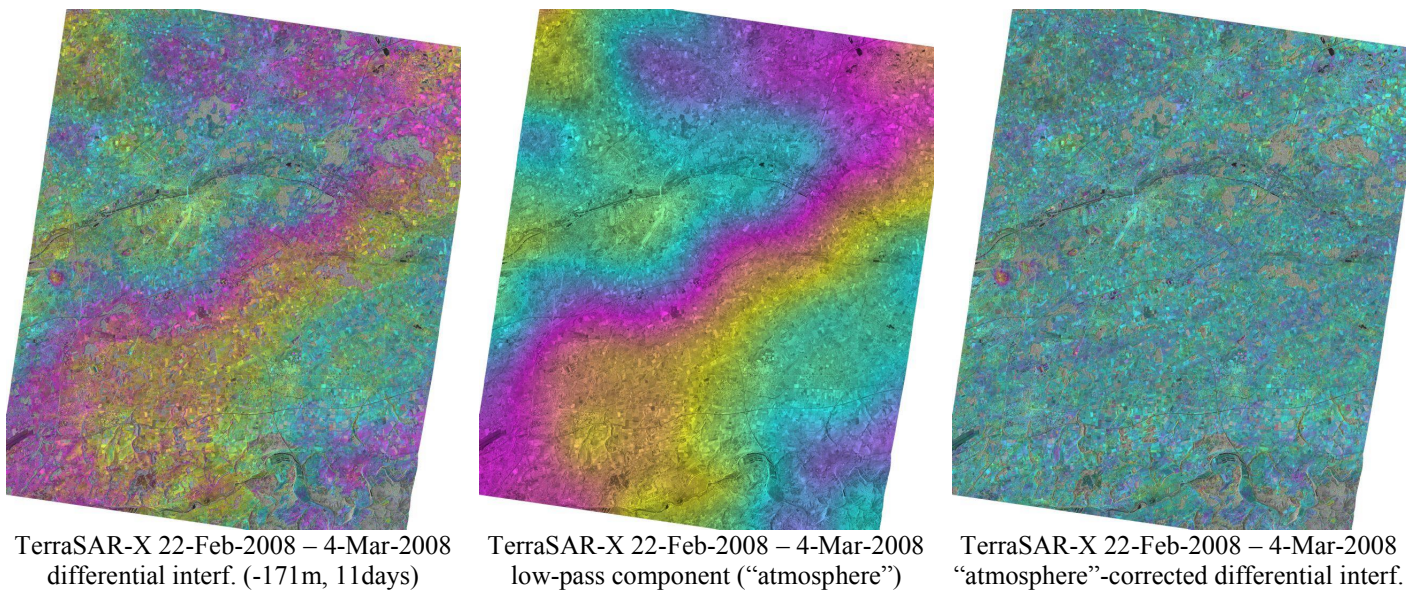


Figure 1 Example for survey differential interferogram

One important observation in the full-area results is that the coherence reduces significantly for longer intervals (see Figure 2). Furthermore, there is more deformation which increases phase gradients for longer intervals which can cause phase unwrapping problems. The coherence increase is not very pronounced though for the first 3 pairs. The 33-day pair 11-Feb-2008 to 15-Mar-2008 still shows intermediate coherence levels over most fields. This is a clear indication that the seasonal effect is indeed important. This observation is further confirmed by investigating a time series of short interval pairs between the consecutive acquisitions, i.e. covering 11 and 22 day intervals (see Figure 3). While bright tones in Figure 3 to the left indicate generally high coherence values over the fields for the February to mid March pairs, the dark tones in Figure 4 to the right indicate low coherence over many fields for the intervals in mid March to May. There are exceptions though also during this period. Some fields show for some intervals intermediate to high coherence. Our understanding is that this behavior relates to the vegetation cover and the cultivation of the fields.

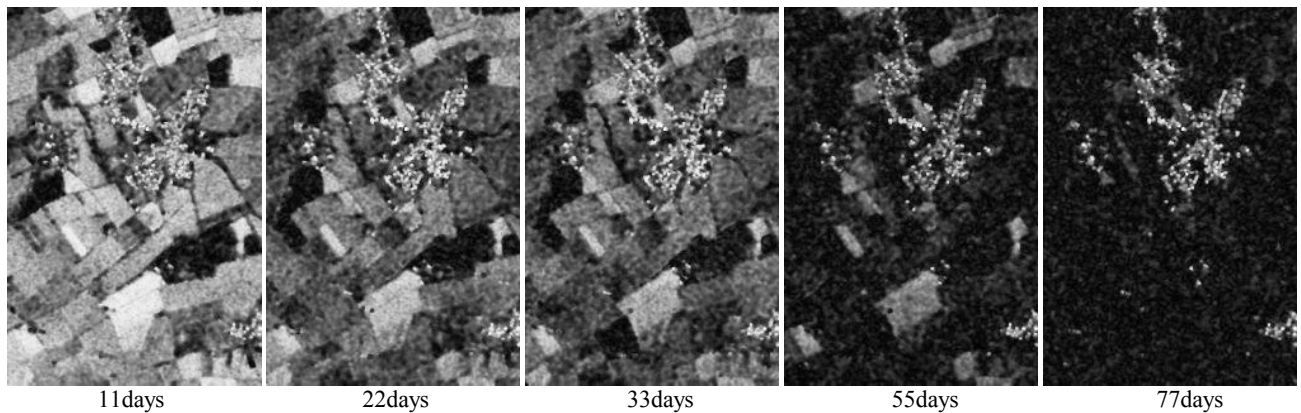


Figure 2. TerraSAR-X coherence for increasing time intervals relative to the master image on 11-Feb-2008. A linear gray scale between 0.0 and 1.0 coherence is used.

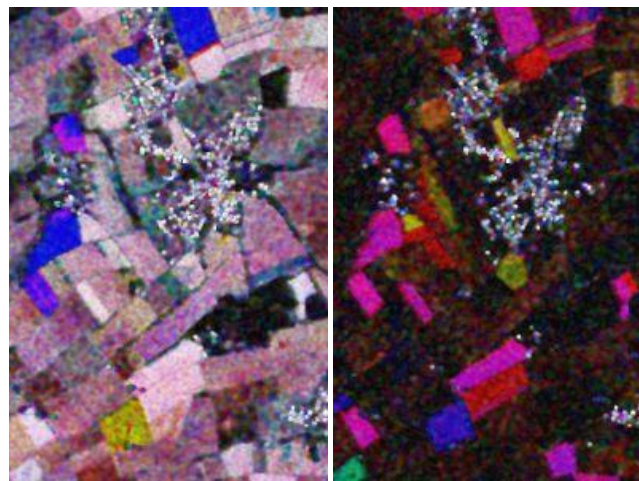


Figure 3. TerraSAR-X short interval coherence composites. Image to the left red: 11-Feb/22-Feb, green: 22-Feb/4-Mar, blue: 4-Mar/15-Mar. Image to the right: red: 15-Mar/6-Apr, green: 6-Apr/28-Apr, blue: 28-Apr/9-May. For each channel a linear scale between 0.0 and 1.0 coherence is used.

Because of these observations, it was then decided to use primarily differential interferograms for a series of consecutive intervals for the further analysis, i.e. A-B, B-C, C-D, etc. For the late winter pairs these 11 or 22-day differential interferograms could be unwrapped without too significant problems. The unwrapping was more challenging for some of the later pairs. In the following some quantitative results are shown for two smaller sub-areas that include important deformation. Phase unwrapping was checked and improved until a satisfactory result was achieved. A minimum-cost-flow unwrapping technique was used. The unwrapped phases were then also summed up to cover longer intervals. As a result a series of deformation maps (A-B, A-C, A-D, etc.) was generated. Over time the spatial coverage reduces more or less to built-up areas (houses, roads, etc.). A local spatial reference point within the section was used. No atmospheric phase was subtracted.

The selected Section 1 is of interest as it includes man-made mine waste heaps which show phase because of deformation as well as because of inaccurate reference heights (outdate DEM) and as it includes an area with relatively slow (max. 20mm/month) temporally most likely quite uniform deformation.

The unwrapped phases include the entire atmospheric path delay effects. In this investigation no atmospheric phase was subtracted in order to avoid shifting deformation phase into the atmospheric component. The unwrapped phases for the incremental intervals were then set to zero for a spatial reference point, summed up, converted to deformation values (line-of-sight as well as vertical component

were calculated), and geocoded. The resulting series of deformation values relative to 11-Feb-2008 is shown in Figure 4. With increasing time interval the spatial coverage reduces.

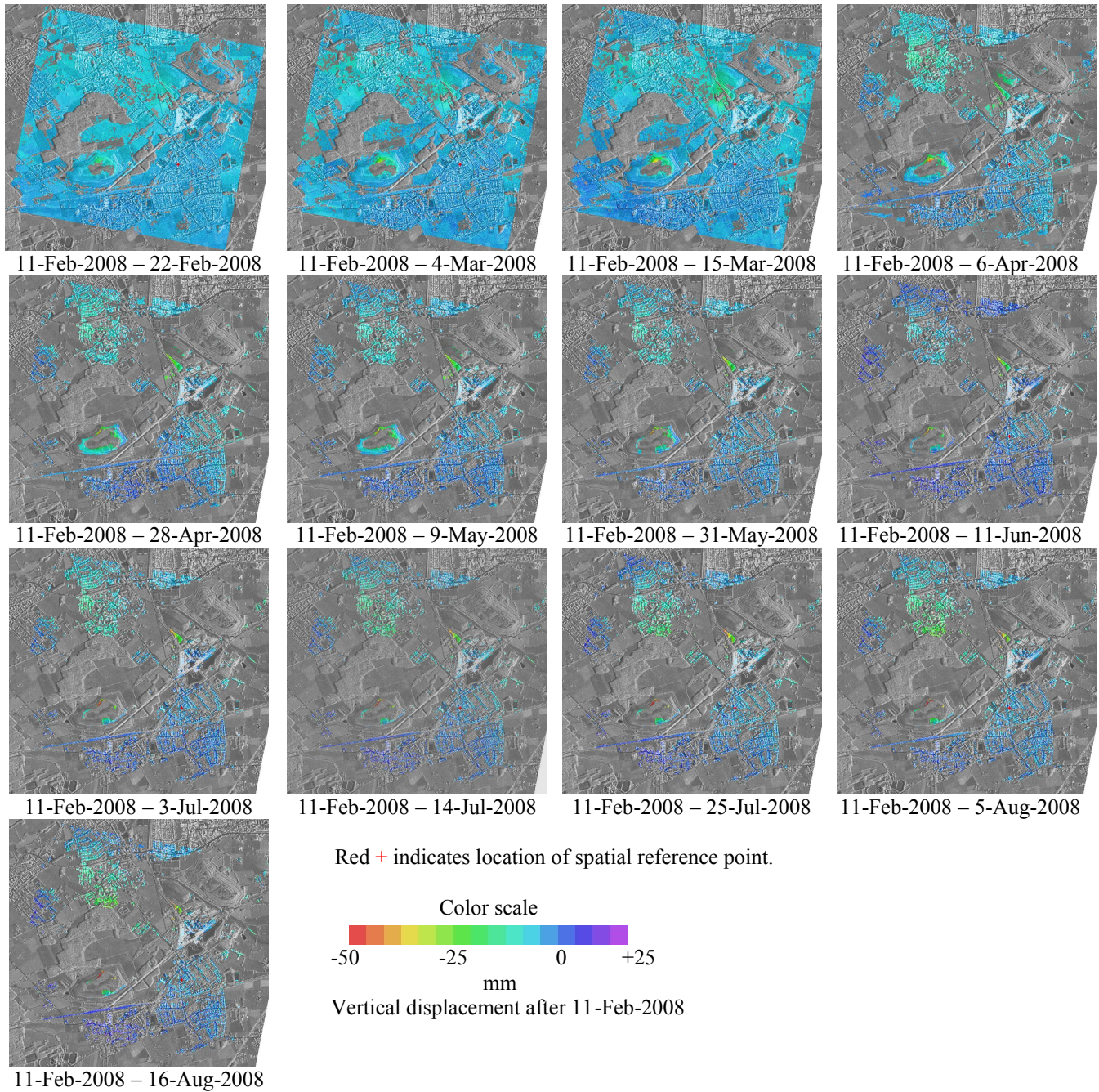


Figure 4 Deformation time series from TerraSAR-X DINSAR for Section 1.

The Section 2 is of interest as it includes an active mining area with significant subsidence. The processing done corresponds to that for Section 1. The resulting series of deformation values relative to 11-Feb-2008 is shown in Figure 5. Again the spatial coverage reduces with increasing time interval.

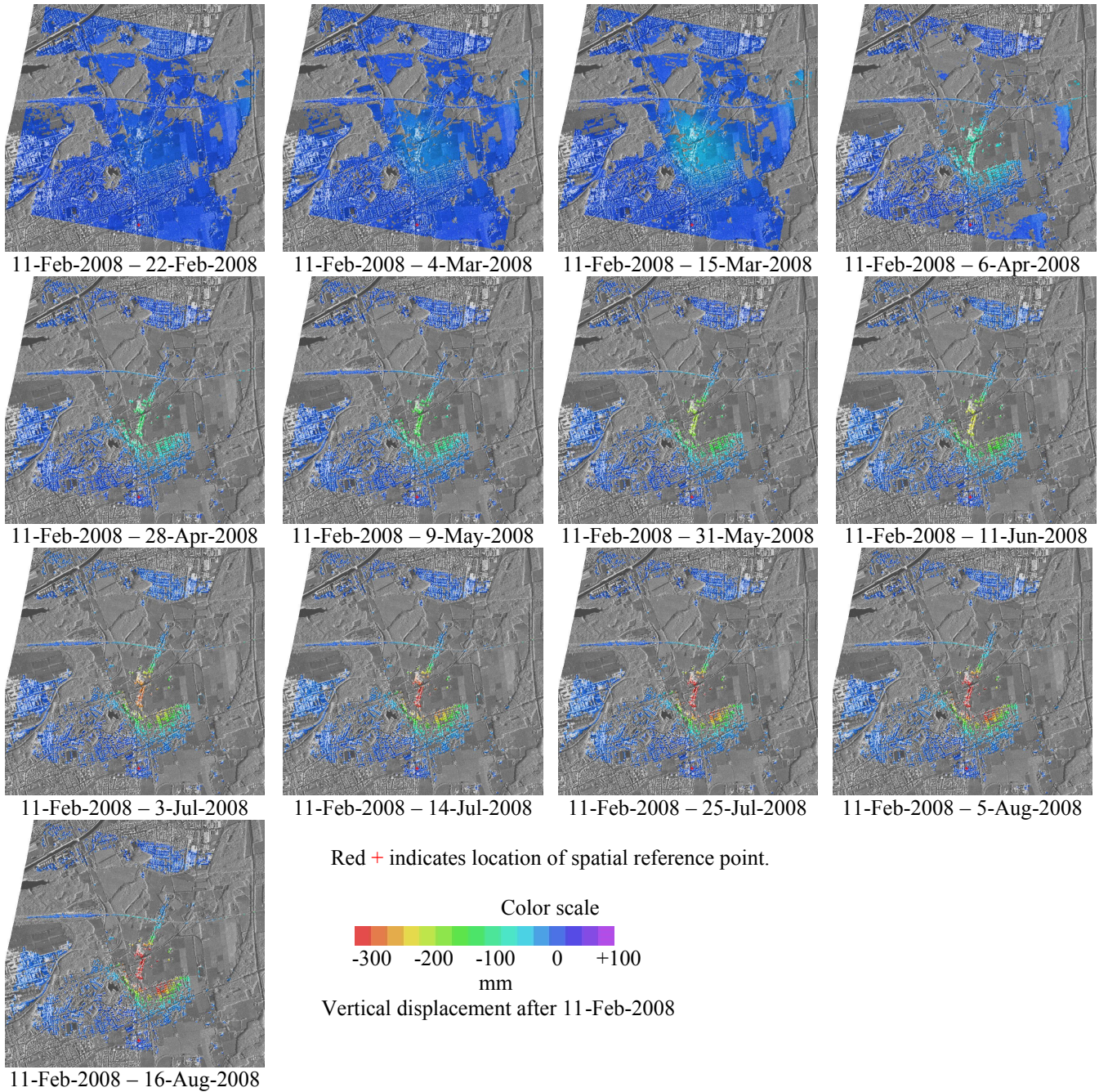


Figure 5 Deformation time series from TerraSAR-X DINSAR for Section 2.

5. Evaluation of different height references and geocoding verification

Initially we used the SRTM 3" DEM heights as reference for the differential interferograms. Overall this works quite well because (1) the terrain is overall quite flat and (b) the baselines are all relatively short. So the “noise” of the SRTM DEM which would cause significant problems in the case of baselines > 600m is not really very relevant.

Nevertheless, some local problems are observed so. There are some new mine waste heaps made from excavation material which are not correctly indicated in the SRTM DEM as they were established or its size increases after the Shuttle Mission. Furthermore, these hills have quite steep slopes and so the 90m resolution of the SRTM DEM is not fully satisfactory.

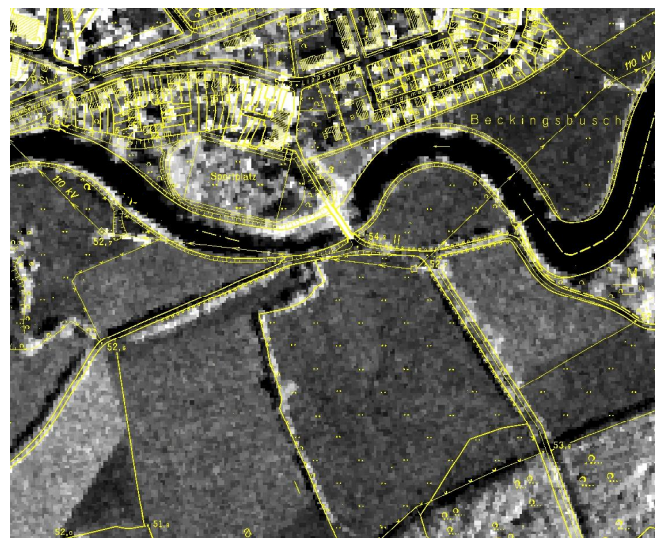
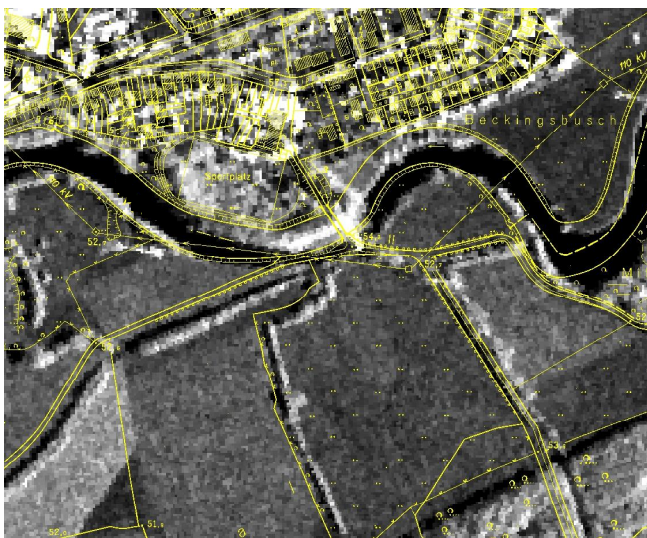
As an alternative with a much higher spatial resolution we tested the NEXTMap DTM. The NEXTMap DTM is based on significantly newer data and so it includes all the relevant hills. Overall it performs

better than the SRTM DEM, but there remain some local topographic phases in the differential interferograms for the hill slopes. Maybe this is partly because of a slight mismatch in the co-registration between the DEM heights and the SAR data. A difficulty is also that the NEXTMap DTM is a terrain model, i.e. it contains the ground surface heights, while the scattering also originates from vegetation and buildings, which may cause additional local geocoding problems in forest and urban areas.

Based on the TerraSAR-X interferometric data we also generated a height reference. One important advantage of this approach is that it assures a perfect geometric match between DEM and SAR data. Difficulties on the other hand are areas of low coherence and that there is also deformation and atmospheric phase. To minimize the effect of deformation and atmosphere we combined two subsequent interferograms both for an 11 day interval. Taking the phase difference all uniform deformation is compensated and only accelerated deformation causes some errors. Furthermore, the pair was such that the two baselines added up to a longer effective baseline around 330m, which reduces the atmospheric errors.

The three different DEMs used as height reference and their performance for a specific differential interferogram (with a 171m perpendicular baseline) are shown in Figure 7. Please notice that the phase visible in the differential interferogram with the TerraSAR-X DINSAR height reference for the newer mine waste heaps relates to deformation of the hill and not to an error in the height reference (as confirmed by other pairs with different baselines).

For an adequate validation of TerraSAR-X interferometric results a precise geocoding is necessary. A DEM is used for geocoding. For geocoding using a mosaic of SRTM-X (1'') and SRTM-C (3'') DEM absolute geocoding accuracies of about 25m in range and of about 8m in azimuth are only reachable for TerraSAR-X data. With high resolution NEXTMap DTM it is possible to reach accuracies of about 3m. Figure 6 show results of geocoding verification using digital topographic maps. Additional artificial corner reflectors were installed to TerraSAR-X acquisitions in the mining area for determination of geocoding accuracy.



SRTM DEM geocoded TerraSAR-X data

NEXTMAP DTM geocoded TerraSAR-X data

Figure 6 Verification of geocoding accuracy using topographic map DK5

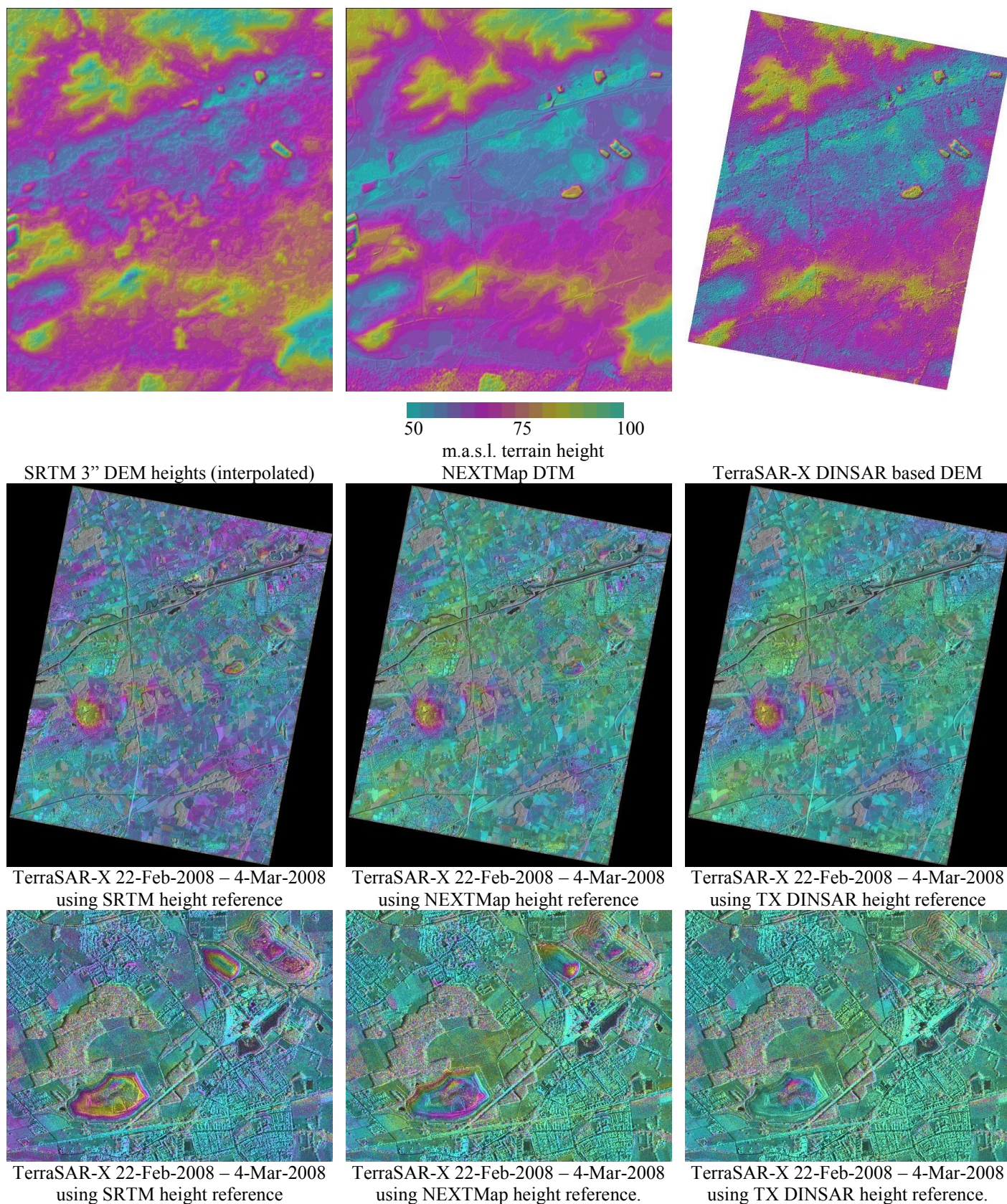


Figure 7 Three different DEM references used (top line), and related differential interferograms obtained for a pair with a 171m baseline (larger area view in the center line) and detailed view of area with newer man-made mine waste heaps (bottom line).

6. Deformation monitoring using Interferometric Point Target Analysis

The Interferometric Point Target Analysis (IPTA) is GAMMA’s implementation of “Persistent Scatterer Interferometry” (PSI). It is a method to exploit the temporal and spatial characteristics of interferometric signatures collected from point targets to accurately map surface deformation histories, terrain heights, and relative atmospheric path delays. The use of targets with point like scatter characteristics has the advantage that there is much less geometric decorrelation. This permits phase interpretation even for large baselines above the critical one. Consequently, more image pairs may be included in the analysis. Important advantages are the potential to find scatterers in low-coherence areas and that interferometric image pairs with large baselines may be included in the analysis. Finding usable points in low-coherence regions fills spatial gaps in the deformation maps while the ability to use large baselines improves the temporal sampling. For a more detailed discussion of the point target based interferometric technique used see [1].

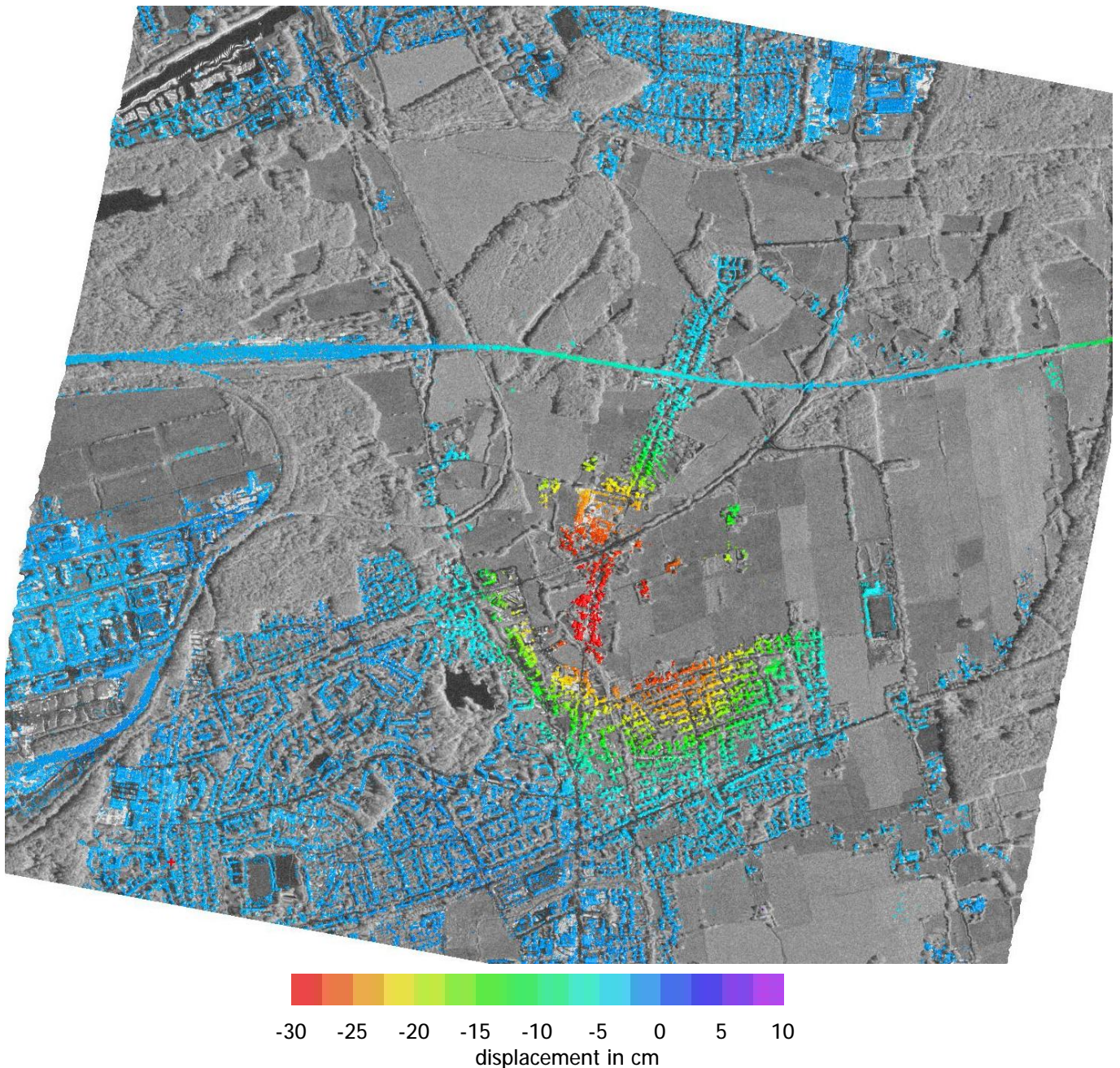


Figure 8 Line-of-sight surface deformation between 11-Feb-2008 and 21-Oct-2008 derived from TerraSAR-X data series in an IPTA processing over an active mining area in Germany.

The specific IPTA processing sequence used in the present case was somewhat adapted to the specific nature of the deformation pattern. The mining related deformation includes high deformation rates with significant spatial deformation gradients. In the past PSI was not very successful under these conditions. To optimise the processing for the case of high deformation gradients and non-uniform motion we worked primarily with a multi-reference stack that included pairs with shorter time intervals (11- to 44-days). For these shorter interval pairs spatial phase unwrapping for the point network was possible. Most likely the quite good point density found for the TerraSAR-X data and the high spatial resolution of the TerraSAR-X data were also relevant factors contributing significantly to the result achieved.

Figure 8 shows the line-of-sight deformation between 11-Feb-2008 and 21-Oct-2008. Subsidence values larger than 30cm were observed in the centre of the subsidence trough. Overall a result was obtained for more than 100'000 points for this area which is approximately 10km² and which includes a significant fraction of vegetated area.

The validation of the result is ongoing. First comparisons (Figure 9) show good correspondence with in-situ measurements for both time series and profiles. Even very fast non-linear movements at point 74141 with maxima of 9cm per month were successfully measured. But for individual IPTA points temporal phase unwrapping was incorrect for few fractions of time, see point 74226. Variations of direction of vertical deformation (subsidence, uplift) at individual points can be measured due to used multi-reference stack.

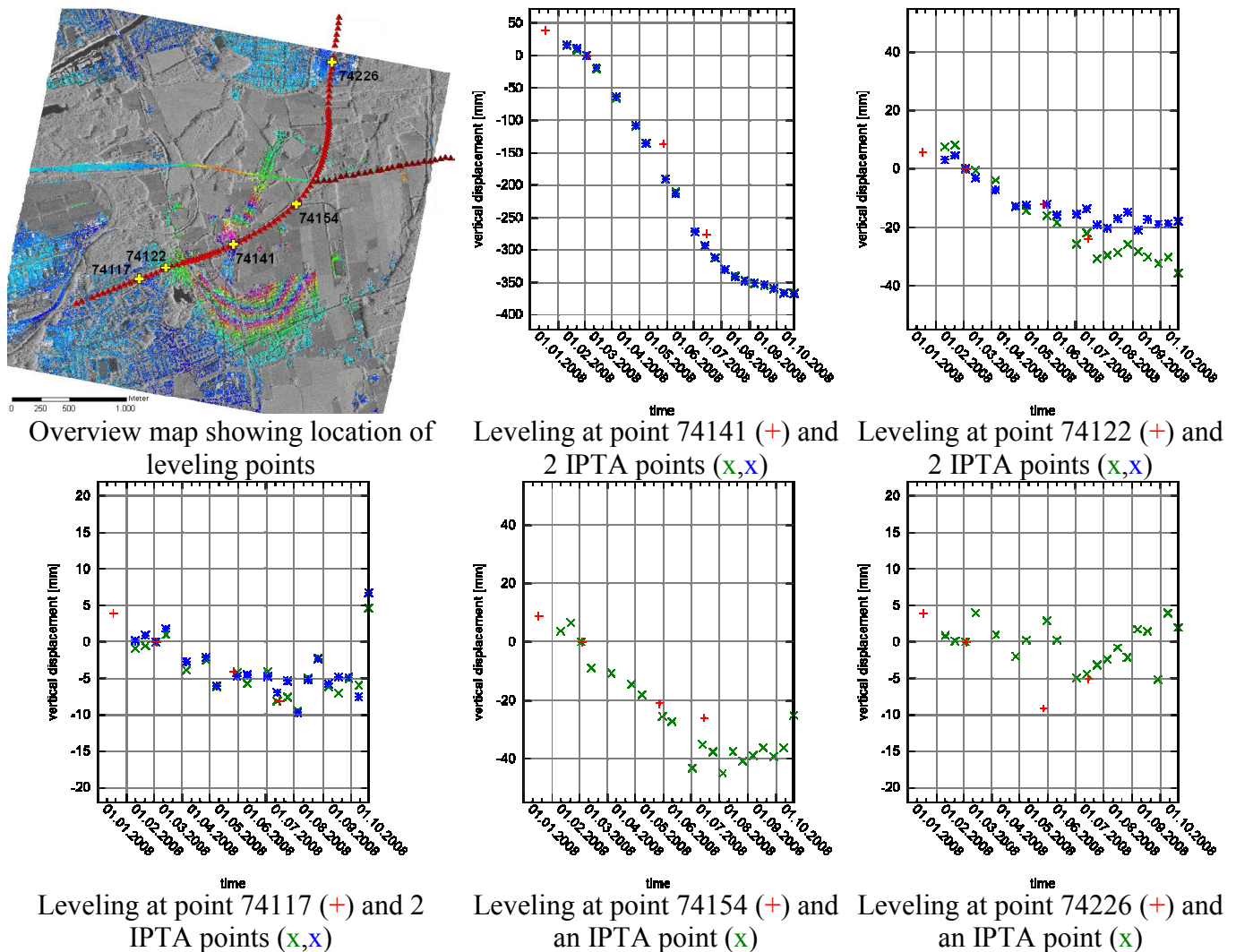


Figure 9 Initial validation results.

7. Conclusions

Results of the DINSAR and IPTA analysis were presented.

During winter months good coherence is observed for much of the area. Phase unwrapping is not too problematic in this case, permitting a quantitative interpretation of the data with respect to terrain height and deformation. Atmospheric path delay effects are the main error in the deformation estimation.

Later on in the year when there is more significant vegetation and change (cultivation) on the fields the coherence reduces significantly. This is even the case for 11-day intervals, but even more so, for longer intervals (22-days, 33-days, ...). Strong multi-looking of the complex differential interferogram followed by unwrapping can still be used to successfully determine and compensate orbital phase trends. Nevertheless, spatial phase unwrapping does no longer work easily. The best chances are to consider subsequent short intervals. But even for these phase unwrapping gets difficult for the late spring and summer pairs because of (a) large areas with low coherence and (b) higher deformation gradients for some 22-day intervals.

For two smaller areas the phase unwrapping problem was carefully addressed and solved. The unwrapped phases were then summed up over time resulting in a series of deformation maps relative to the starting date. Stronger deformation can clearly be identified and the relative error from atmospheric path delays is relatively low. For slow deformation (<1cm/year), nevertheless, there is confusion between deformation phase and atmospheric effects. No special attempts to address this were conducted in this analysis. The spatial coverage of the deformation maps reduces over time until mainly the built up areas remain. In some cases this may be sufficient to catch a specific deformation pattern (subsidence cone) in other cases not. Furthermore, 3 different DEMs were evaluated with respect to differential interferometry.

Finally Persistent Scatterer Interferometry was successfully applied to the available TerraSAR-X data stack. The result achieved was very satisfactory as it was possible to map fast non-uniform deformation at good accuracy, as confirmed by initial comparisons with in-situ measurements.

8. References

- [1] Wegmüller U., C. Werner, T. Strozzi, and A. Wiesmann, "Multi-temporal interferometric point target analysis", in *Analysis of Multi-temporal remote sensing images*, Smits and Bruzzone (ed.), Series in Remote Sensing, Vol. 3, World Scientific (ISBN 981-238-915-61), pp. 136-144, 2004.

9. Acknowledgment

This work was supported by the RAG R&D project GEOMON (FE0572-0000) and RFCS2007-Project PRESIDENCE (RFCR-CT-2007-00004) of the Research Programme of the Research Fund for Coal and Steel (RFCS-CT). TerraSAR-X data used in this work are provided by DLR in the frame of the TerraSAR-X Pre-launch AO Project GEO_165 (PI Urs Wegmüller).